

Laser Raman and X-ray photoelectron spectroscopy of phosphorus containing diamond-like carbon films grown by pulsed laser ablation methods

G.M. Fuge, P.W. May*, K.N. Rosser, S.R.J. Pearce, M.N.R. Ashfold

School of Chemistry, University of Bristol, Cantock's Close, Bristol BS8 1TS, UK

Abstract

Mechanically hard, electrically conducting diamond-like carbon (DLC) films containing 0 to ~26 at.% phosphorus have been deposited on both Si and quartz substrates by pulsed laser ablation of graphite/phosphorus targets (containing varying percentages of phosphorus), at a range of substrate temperatures ($T_{\text{sub}} = 25\text{--}400\text{ }^{\circ}\text{C}$), in vacuum. Laser Raman spectra (514.5 nm excitation wavelength) of the as-deposited films yield the band maxima and relative intensities of the D and G peaks ($I(\text{D})$ and $I(\text{G})$, respectively), as a function of T_{sub} , P:C ratio and incident laser fluence, F . Nanocrystalline graphitisation was deduced to occur at higher substrate temperatures, consistent with previous results for undoped DLC and CN_x films. P containing DLC films deposited at lower T_{sub} values exhibit higher $I(\text{D})/I(\text{G})$ ratios than the corresponding undoped DLC films. Measured trends in G-peak positions and $I(\text{D})/I(\text{G})$ ratios are consistent with values for the C-sp³ content obtained by deconvoluting the C 1s peak in the corresponding X-ray photoelectron spectra. XPS also reveals a decrease in P content in films grown at higher T_{sub} and at higher F , suggesting that P atoms are more mobile than C atoms, and thus less strongly accommodated, during the film growth process.

© 2003 Elsevier B.V. All rights reserved.

Keywords: Diamond-like carbon (DLC); Pulsed laser deposition (PLD); Mechanical properties; Film characterisation

1. Introduction

Doped diamond-like carbon (DLC) films have been extensively studied using N as the dopant atom to produce CN_x films [1–10]. Interest in these films increased considerably given the outstanding physical properties predicted for $\beta\text{-C}_3\text{N}_4$ – e.g. hardness values comparable to diamond combined with high toughness [11,12], together with excellent tribological, chemical and electrical properties. Phosphorus is an alternative dopant to nitrogen, but the analogous P_4C_3 compound is predicted to have a structure and characteristics very different from those of $\beta\text{-C}_3\text{N}_4$ [13]. Investigating P incorporation into DLC films is clearly of interest, though the resulting P-DLC thin films may be expected to exhibit different properties to CN_x films given phosphorus' greater preference for tetrahedral coordination. Previous studies have shown that the incorporation of

$\leq 1\%$ P into DLC films reduces their resistivity by 6–7 orders of magnitude [14]. Other groups have introduced larger amounts of P into DLC films and observed similar increases in room temperature conductivity, but also noted a higher graphitic content [15–18]. The Bristol group has used CH_4/PH_3 gas mixtures and RF plasma chemical vapour deposition (CVD) methods to produce amorphous films with P:C ratios $\leq 3:1$. Given their high P content, it is not really appropriate to envisage such films as P doped DLC and, consequently, they have been termed 'amorphous carbon phosphide' [19,20]. These films typically contain ~10% H – though this can be reduced by increasing the DC bias during deposition – and are sensitive to aerial oxidation (resulting in cracking and delamination).

Pulsed laser ablation (PLA) from solid targets composed of mixtures of C and P and subsequent deposition on a suitable substrate offers an alternative route to producing P-DLC thin films, free of H, and with controllable P/C ratios. The aim of the present work is to investigate properties of P-DLC films deposited by

*Corresponding author. Tel.: +44-117-928-9927; fax: +44-117-9251295.

E-mail address: paul.may@bris.ac.uk (P.W. May).

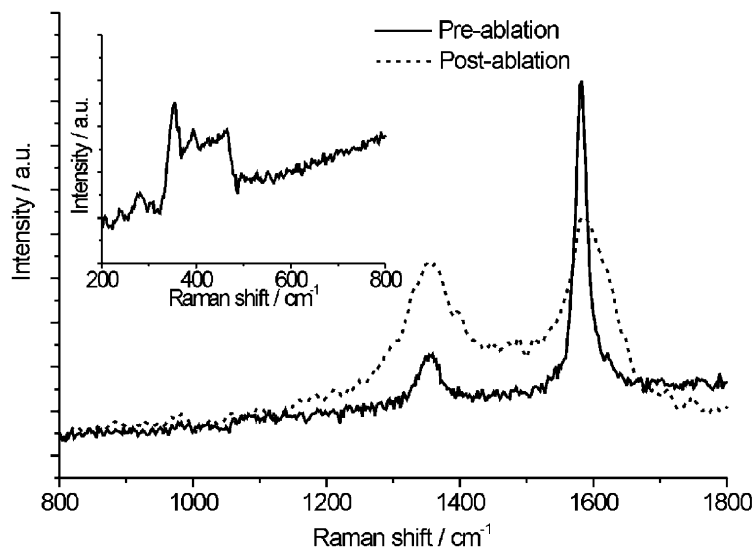


Fig. 1. Laser Raman spectra (514.5 nm) of a 10% P:C target pre- and post- exposure to ArF laser radiation ($F=4 \text{ J cm}^{-2}$, 10 Hz, 20 min exposure). The sharp D and G peaks at $\sim 1350 \text{ cm}^{-1}$ and $\sim 1580 \text{ cm}^{-1}$, respectively, – which are characteristic of crystalline graphite – are noticeably broader in the spectrum of the post-ablated target. The inset shows a vertically expanded view of the $200\text{--}800 \text{ cm}^{-1}$ region, confirming the presence of P (via the peaks between 320 and 490 cm^{-1}) and the lack of features associated with C–P bonding (by the absence of features in the $650\text{--}770 \text{ cm}^{-1}$ range).

this method, as a function of P:C ratio and process conditions.

2. Experimental

P-DLC films were deposited by PLA of phosphorus/carbon targets as a function of substrate temperature, T_{sub} , (in the range $25\text{--}400 \text{ }^\circ\text{C}$), laser fluence and target P:C ratio. Targets were prepared from intimately mixed samples of graphite and red phosphorus powder containing, respectively, 10%, 20%, 30% and 50% by weight P. Each was fabricated into a 52-mm diameter disk using a hydraulic press with maximum pressure of 560 kN, and subsequently polished to obtain a smooth, flat surface. The target of choice was then mounted on a rotating stage and situated inside a stainless steel chamber evacuated to $<10^{-6}$ Torr by a turbomolecular pump. The output of an ArF (193 nm) excimer laser (Lambda-Physik, Compex 201) operating at 10 Hz was steered by two mirrors through a circular aperture and a fused silica lens (450 mm focal length), and then through a quartz window in the chamber onto the target. The focal spot size on the target was $\sim 1 \text{ mm}^2$ (yielding typical incident fluences, F , in the range $4\text{--}12 \text{ J cm}^{-2}$). Films were deposited on both n-type single crystal (100) Si and quartz substrates (approx. 1 cm^2 in area). These were mounted on the target surface normal, 80 mm distant from the focal spot, on a purpose-designed holder positioned immediately in front of a compact 15 W light-bulb heater that allowed deposition at any user-selected $T_{\text{sub}} \leq 400 \text{ }^\circ\text{C}$.

The deposited films were analysed by laser Raman spectroscopy (Renishaw 2000 system, 514.5 nm excitation wavelength), X-ray photoelectron spectroscopy (XPS) (Fisons Instruments VG Escascope equipped with a Mg $K\alpha$ (1253.6 eV) source and an analyser energy resolution of approx. 0.9 eV) and scanning electron microscopy (JEOL JSM 5600 LV scanning electron microscope). Spectroscopic ellipsometry was performed on films deposited on Si (Woollam VASE ellipsometer), at five incident angles between 55 and 75° , yielding values for Δ and Ψ over the spectral range of $200\text{--}1000 \text{ nm}$. Film optical constants (n , k) and the film thickness were calculated using a model of amorphous semiconductor on 0.5-mm thick crystalline Si, with the semiconductor layer described using the Tauc–Lorentz model [21]. A limited number of films deposited on quartz substrates were subjected to four-point probe analysis using an inter-probe separation of 3 mm.

3. Results and discussion

Fig. 1 displays Raman spectra (514.5 nm excitation) of a 10% P in C target, pre- and post-ablation, in the wavenumber range $800\text{--}1800 \text{ cm}^{-1}$ together with, as an inset, the $200\text{--}800 \text{ cm}^{-1}$ region of the spectrum recorded from the virgin target. Features evident in the range $320\text{--}490 \text{ cm}^{-1}$ confirm the presence of P in the target [22,23]. Amorphous red phosphorus consists of P_7 and P_9 cages arranged to form pentagonal tubes in paired layers; P_9 cages are considered responsible for

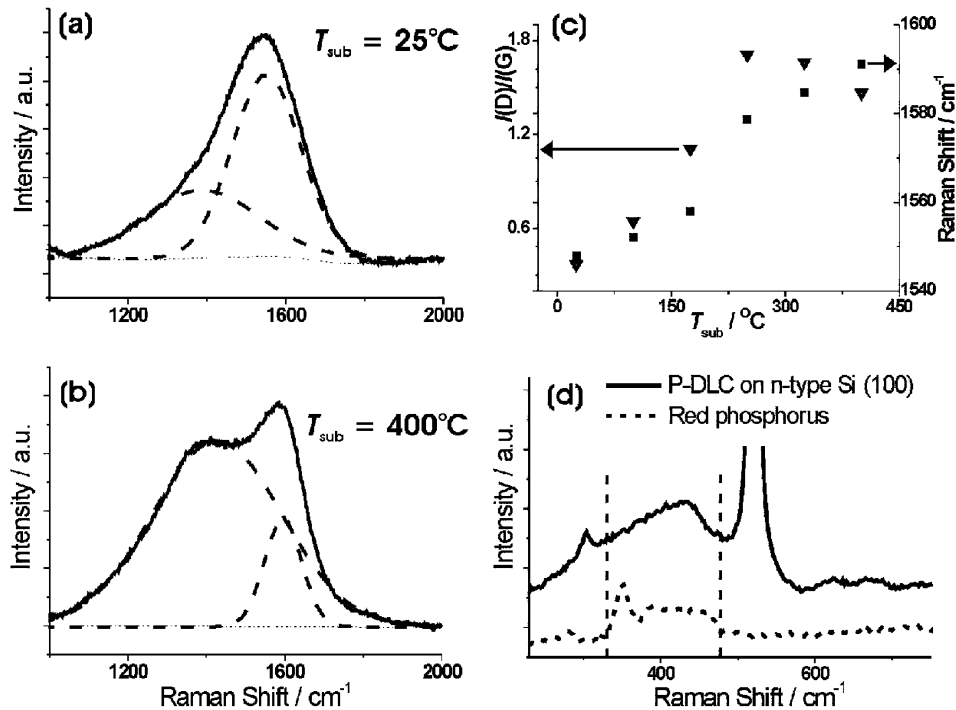


Fig. 2. Details from the Raman spectra (514.5 nm excitation) of P-DLC films grown on n-type Si (100) substrates by PLA of a target comprising 10% P in C (by weight) in vacuum at $T_{\text{sub}}=25^\circ\text{C}$ (a) and 400°C (b). Each has been fitted in terms of two independent Gaussian functions (solid curves), while the dashed line at $y\sim 0$ shows the residuals of the fit. Panel (c) illustrates the T_{sub} dependence of the $I(\text{D})/I(\text{G})$ ratio deduced from such deconvolutions (\blacktriangledown), and the G width (\blacksquare). (d) shows a comparison of the $\sim 400\text{ cm}^{-1}$ feature in the Raman spectra of a P-DLC film grown at $T_{\text{sub}}=25^\circ\text{C}$ by PLA of a 50% P in C target in vacuum with that obtained from a pure red phosphorus sample. The two spectra have been offset vertically for clarity.

the sharp peak at $\sim 350\text{ cm}^{-1}$ [22,23]. The peaks appearing in the main spectra are characteristic of graphitic carbon. The G mode of graphite (approx. 1580 cm^{-1}) involves an E_{2g} symmetrical bond stretching motion of pairs of C sp^2 atoms, while the D band (approx. 1350 cm^{-1}) is attributed to the breathing mode of six-membered rings. The small relative intensity of the D peak and the narrow full width half maximum (FWHM) of the G peak are both indicators of the presence of high quality graphite in the virgin target, the crystallinity of which is degraded by the ablation process.

All films produced by 193 nm PLA of such targets were hard, and immune to scratching by steel tweezers. Scanning electron microscopy (SEM) images of the film surface revealed the presence of macroscopic particulates – a characteristic feature of almost all films deposited by pulsed laser deposition [24] – but are otherwise locally featureless, implying that the films are smooth on the scale of tens of nanometres. Ellipsometry showed films deposited at room temperature to be $\sim 30\text{-nm}$ thick ($F\sim 4\text{ J cm}^{-2}$, 20 min deposition), independent of target P:C ratio, implying a deposition rate of $\sim 90\text{ nm h}^{-1}$ or $\sim 2.5\text{ pm}$ per laser shot. The film thickness was found to decrease with increasing T_{sub} from ~ 40

nm ($T_{\text{sub}}=25^\circ\text{C}$, $F\sim 8\text{ J cm}^{-2}$) to $\sim 20\text{ nm}$ ($T_{\text{sub}}=400^\circ\text{C}$, $F\sim 8\text{ J cm}^{-2}$) but to increase with increasing F from $\sim 30\text{ nm}$ ($T_{\text{sub}}=25^\circ\text{C}$, $F\sim 4\text{ J cm}^{-2}$) to $\sim 50\text{ nm}$ ($T_{\text{sub}}=25^\circ\text{C}$, $F\sim 12\text{ J cm}^{-2}$). The film refractive index, n , was seen to be relatively invariant to P content, but to increase gently with increasing fluence (from approx. 2 at $F=4\text{ J cm}^{-2}$ to approx. 2.6 at 12 J cm^{-2}). Previous workers have noted a correlation between refractive index and film hardness, scratch resistance and wear resistance; determining n thus provides one measure of film quality [25].

Fig. 2 shows selected portions of the laser Raman spectra (514.5 nm excitation) of P-DLC films grown on an n-type Si (100) substrate by PLA of a target consisting of 10% P in C ((a) and (b)) and 50% P in C (d), in vacuum. Panels 2(a) and 2(b) highlight the T_{sub} dependence of the broad feature present in the range $1000\text{--}2000\text{ cm}^{-1}$, which, following past procedures, we deconvolute using Gaussian functions into contributions associated with the D and G vibrational modes of graphite. Quantities of interest include the wavenumbers of the G and D band maxima, G_{max} and D_{max} , and the ratio of the peak intensities of the deconvoluted D and G bands, $I(\text{D})/I(\text{G})$. As seen in many other cases [26–30], the introduction of dopant atoms such as N (or, in

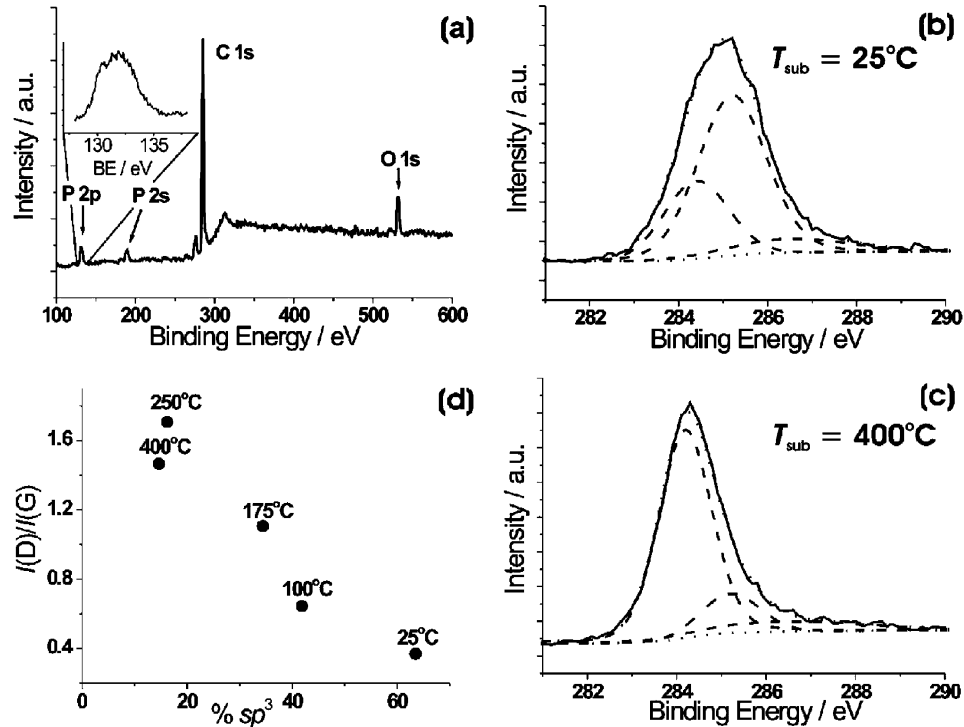


Fig. 3. (a) Overview XPS spectrum (100–600 eV) of a P-DLC film grown at $T_{\text{sub}} = 25^\circ\text{C}$ by PLA of a 10% P in C target. Peaks attributable to P(2s and 2p), C(1s) and O(1s) (from aerial oxidation) are readily identifiable; the inset shows the P(2p) peak in greater detail. (b) and (c) show details of the C(1s) peak in the XPS spectra of films deposited at $T_{\text{sub}} = 25^\circ\text{C}$ and 400°C , together with the respective deconvolutions into three Voigt lineshape functions. (d) shows a plot of $I(\text{D})/I(\text{G})$ ratio (from Fig. 2c) vs. C- sp^3 content for films grown at a range of different T_{sub} values.

this case, P) causes a marked increase in the room temperature $I(\text{D})/I(\text{G})$ ratio compared to that found for a pure DLC film deposited under otherwise identical conditions. Such is traditionally interpreted in terms of an increased propensity for nanocrystalline graphite formation and possible formation of fullerene-like structures in the matrix [4].

Inspecting Fig. 2a and 2b reveals that G_{max} and D_{max} both shift to higher wavenumber with increasing T_{sub} . The $I(\text{D})/I(\text{G})$ ratio also increases with T_{sub} , but shows a higher room temperature value and maximises at somewhat lower T_{sub} than found for pure DLC films grown under otherwise identical conditions. Panel 2(c) summarises these trends with T_{sub} , which mirror those seen previously in the case of N doped DLC films [26]. The observed increases in G_{max} , D_{max} and the $I(\text{D})/I(\text{G})$ ratio with increasing T_{sub} have been interpreted in terms of a shift from amorphous to nanocrystalline film growth [31]. Increasing T_{sub} from 25 to 400°C also leads to a reduction in the FWHM of the G peak from ~ 200 to $\sim 100\text{ cm}^{-1}$ (c.f. approx. 20 cm^{-1} in the spectrum of the virgin target). Such a decrease with respect to increasing T_{sub} signifies an increase in the structural ordering of the graphitic component.

Panel 2(d) compares the $\sim 400\text{ cm}^{-1}$ feature in the Raman spectrum of a P-DLC film grown at room

temperature by PLA of a 50% P in C target in vacuum with that obtained from a pure red phosphorus sample. The two spectra have been offset vertically for clarity. Clearly, the spectrum of the P-DLC film lacks the sharp peak at $\sim 350\text{ cm}^{-1}$, and the maximum of the feature has shifted to higher wavenumber (approx. 430 cm^{-1}). The loss of the 350 cm^{-1} feature, generally attributed to P_9 cages [22,23], is consistent with preferential break-up of the larger cages during the PLA process. The absence of any Stokes shifted feature in the $650\text{--}770\text{ cm}^{-1}$ range is also noteworthy. This is the region in which C–P bond stretching modes would be expected. Since this mode will be Raman active [32], the absence of any such feature in the Raman spectra suggests relatively little C–P bonding in the film and that carbon and phosphorus each prefer to aggregate as localised clusters embedded in an amorphous matrix.

Fig. 3 presents results from XPS analysis of the deposited films. Panel 3(a) shows an overview XPS spectrum (100–600 eV) of a P-DLC film grown by PLA of a 10%P in C target. Peaks attributable to P(2s and 2p), C(1s) and O(1s) (from aerial oxidation) are readily identifiable. Absolute P/C/O ratios were determined by comparing the respective peak areas, A_x , weighted by the appropriate atomic sensitivity factors (i.e. $\text{P:C:O} = A_{\text{P}}(2\text{p})/0.39 : A_{\text{C}}/0.25 : A_{\text{O}}/0.66$). Such

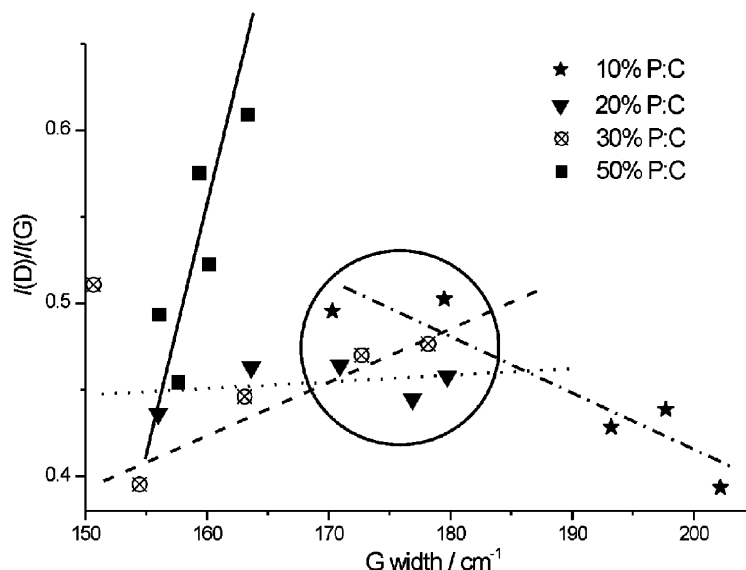


Fig. 4. Plots of $I(D)/I(G)$ ratio versus the FWHM of the G peak for P-DLC films deposited at $T_{\text{sub}} = 25$ °C by PLA of targets with different P:C ratios. The various data points associated with each particular target composition were obtained at different incident laser fluences (F increases from left to right along each tie line). The circle indicates the range of samples tested for electrical conductivity using a four-point probe method.

analyses of P-DLC films showed their stoichiometry to follow that of the target. In the case of P-DLC films deposited at room temperature, for example, PLA of a 10% P in C target yielded films with a P content of ~ 6.5 at.% (i.e. approx. 15% P by weight), while those grown from a 50%P in C target were found to contain ~ 18 at.% P (approx. 36% P by weight). Increasing T_{sub} caused a decline in P content (e.g. falling to approx. 1.5 at.% in the case of films grown from the 10% P in C target at $T_{\text{sub}} = 400$ °C), as did increasing fluence (e.g. from 25 to 18 at.% P in the case of films grown from the 50% P in C target as F was increased from approx. 4 to approx. 12 J cm^{-2}). These compositional data, and the observed decline in film thickness with increasing T_{sub} , are all consistent with a view that P atoms are more mobile than C, and thus less strongly accommodated, during the film growth process.

The P(2p) feature is shown on an expanded scale in Fig. 3a. Its apparently symmetric lineshape is deceptive, since the envelope necessarily contains two spin-orbit components (split by approx. 1 eV [33]) and analysis of the whole set of spectra recorded in the present work indicates that much of the high-energy wing is associated with P–O bonding. Unfortunately, we are unable to attribute any part of the feature specifically to P–C bonding. Analysis of the P(2p) (or P(2s)) XPS peaks thus offers little insight into the extent of P–C bonding in P-DLC films grown by PLA of P/C targets.

As Fig. 3b and 3c show, however, the detailed shape of the C(1s) peak is much more sensitive to the deposition conditions. As in our previous investigation of CN_x thin films [26], we have attempted to deconvolute these lineshapes in order to gain some insight into

the ratio of sp^3 to sp^2 -bonded carbon in the films [34]. We persist with the assumption that the films contain relatively little C–P bonding, and thus model the C(1s) peak in terms of contributions from C- sp^3 , C- sp^2 and C–O bonding only (using Voigt lineshape functions centred at ~ 285.2 eV, 284.4 eV and 286.5 eV, respectively, [35]). Such deconvolutions are illustrated in Fig. 3b and 3c for the respective cases of P-DLC films grown by PLA of a 10% P in C target at $T_{\text{sub}} = 25$ and 400 °C. Analysis of the former suggests a C- sp^3 content of $\sim 64\%$, which has dropped to $\sim 15\%$ at $T_{\text{sub}} = 400$ °C. These percentages correspond to $\text{sp}^3:\text{sp}^2$ ratios of ~ 2.3 and ~ 0.2 , respectively. C- sp^3 content is thus maximised at low T_{sub} . As Fig. 2c showed, growth at low T_{sub} also results in the lowest $I(D)/I(G)$ ratios. Both sets of observations are consistent with the recognised evolution from amorphous carbon towards the formation of islands of nanocrystalline graphite as T_{sub} is increased. As Fig. 3d shows, there is an inverse correlation between $I(D)/I(G)$ ratio and C- sp^3 content for films grown at $T_{\text{sub}} \leq 250$ °C, but this breaks down at yet higher T_{sub} values. This break down can be understood by noting that the $I(D)/I(G)$ vs. T_{sub} plot maximizes at ~ 325 °C. Such trends have been observed, and explained, previously [26,31]. Above this temperature, the measured $I(D)/I(G)$ ratio is found to vary inversely with the sp^2 cluster size (L_a) [36] – consistent with the turn-over at the highest T_{sub} value shown in Fig. 3d.

Fig. 4 provides further illustrations of the sensitivity of the P-DLC film structure to P/C ratio and to the incident laser fluence used during their preparation. The data in this figure were derived by laser Raman analysis

of a series of films deposited on room temperature Si substrates. These analyses revealed F and %P dependent trends in both the $I(D)/I(G)$ ratio and the G peak width. In the case of films grown from the 10% P in C target, for example, the $I(D)/I(G)$ ratio is seen to decrease, and the G width to increase, with increasing F in a manner reminiscent of undoped DLC (i.e. of an amorphous carbon film with relatively high sp^3 content). Very different behaviour is observed in the case of films grown by PLA of the 50% P in C target: in this case $I(D)/I(G)$ increases with increasing F and the G width is comparatively narrow (i.e. characteristics more typical of nano-crystalline graphitic carbon). Films grown from targets with intermediate P:C ratios exhibit trends in $I(D)/I(G)$ and in G width that fall sensibly within these two extremes. One motivation for attempting P incorporation into DLC films would be to investigate its effect on the electronic properties of the film. Unfortunately, as Figs. 2–4 all show, varying the P content, T_{sub} and even the laser fluence incident on the target all influence the degree of graphitisation within the film, making it almost impossible to isolate effects that are solely and unambiguously attributable to the presence of P atoms. Nonetheless, four-point probe tests were carried out on a number of films grown on quartz substrates, and exhibiting $I(D)/I(G)$ ratios and G peak widths that fall within the region enclosed by the circle in Fig. 4. From these measurements, we calculate a resistivity of $\sim 20 \Omega \text{ cm}$, which appears to decrease slowly with increasing P content, and is some six orders of magnitude smaller than that found for tetrahedral amorphous carbon (ta-C) films grown by PLA of a pure graphite target under otherwise identical conditions.

4. Conclusions

PLA has been used to deposit mechanically hard, electrically conducting P-DLC films containing 0–26 at.% P on Si and quartz substrates. Laser Raman analysis and XPS have been used to demonstrate that both the C- sp^3 fraction and the P content are influenced by the chosen values of T_{sub} , P:C ratio in the target (and thus in the deposited film) and the incident laser fluence. Such flexibility and control may offer a route to tailoring P-DLC films for a specific application, such as a mechanical wear-resistant coating or in electronic devices.

Acknowledgments

We are grateful to Dr Manish Chhowalla (Cambridge University) for help with target preparation, to J. Filik and to the staff of the Mechanical and Electronic workshops at the School of Chemistry for their help with and support of this work, and to the EPSRC for financial support.

References

- [1] F. Muhl, J.M. Mendez, *Diamond Relat. Mater.* 8 (1999) 1809, and references therein.
- [2] Y. Zhang, Z. Zhou, H. Li, *Appl. Phys. Lett.* 68 (1996) 634.
- [3] E. Gyorgy, V. Nelea, I.N. Mihailescu, A. Perrone, H. Pelletier, A. Cornet, et al., *Thin Solid Films* 388 (2001) 93.
- [4] A.A. Voevodin, J.G. Jones, J.S. Zabinski, L. Huttman, *J. Appl. Phys.* 92 (2002) 724.
- [5] N. Hellgren, K. Macak, E. Broitman, L. Hultman, J.-E. Sundgren, *J. Appl. Phys.* 88 (2001) 524, and references therein.
- [6] D.-H. Lee, H. Lee, B. Park, D.B. Poker, L. Riester, *Appl. Phys. Lett.* 70 (1997) 3104.
- [7] P. Merel, M. Chaker, M. Tabbal, M. Moisan, *Appl. Phys. Lett.* 71 (1997) 3814.
- [8] S.E. Rodil, W.I. Milne, J. Robertson, L.M. Brown, *Appl. Phys. Lett.* 77 (2000) 1458.
- [9] A.C. Ferrari, S.E. Rodil, J. Robertson, *Phys. Rev. B* 67 (2003) 155306.
- [10] J. Robertson, *Mater. Sci. Eng. R* 37 (2002) 129.
- [11] A.Y. Liu, L. Cohen, *Science* 245 (1989) 841.
- [12] A.Y. Liu, L. Cohen, *Phys. Rev. B* 41 (1990) 10 727.
- [13] F. Claeysens, N.L. Allan, P.W. May, P. Ordejón, J.M. Oliva, *Chem. Commun.* (2002) 2494.
- [14] V.S. Veerasamy, G.A.J. Amaratunga, C.A. Davis, A.E. Timbs, W.L. Milne, D.R. McKenzie, *J. Phys.: Condens. Matter.* 5 (1993) 169L.
- [15] M.-T. Kuo, P.W. May, A. Gunn, M.N.R. Ashfold, R.K. Wild, *Diamond Relat. Mater.* 9 (2000) 1222.
- [16] M.M. Golzan, D.R. McKenzie, D.J. Miller, S.J. Collocott, G.A.J. Amaratunga, *Diamond Relat. Mater.* 4 (1995) 912.
- [17] S.M. Mominuzzaman, T. Soga, T. Jimbo, M. Umeno, *Diamond Relat. Mater.* 10 (2001) 1839.
- [18] S.M. Mominuzzaman, H. Ebisu, T. Soga, T. Jimbo, M. Umeno, *Diamond Relat. Mater.* 10 (2001) 984.
- [19] S.R.J. Pearce, P.W. May, R.K. Wild, K.R. Hallam, P.J. Heard, *Diamond Relat. Mater.* 11 (2002) 1041.
- [20] S.R.J. Pearce, J. Filik, P.W. May, R.K. Wild, K.R. Hallam, P.J. Heard, *Diamond Relat. Mater.* 12 (2003) 979.
- [21] G.E. Jellison Jr, V.I. Merkulov, A.A. Puzosky, D.B. Geohegan, G. Eres, D.H. Lowndes, et al., *Thin Solid Films* 377 (2000) 68.
- [22] D.J. Olego, J.A. Baumann, M.A. Kuck, R. Schachter, C.G. Michel, *Solid State Commun.* 52 (1984) 311.
- [23] G. Fasol, M. Cardona, W. Hönl, H.G. von Schnering, *Solid State Commun.* 52 (1984) 307.
- [24] M.N.R. Ashfold, F. Claeysens, G.M. Fuge, S.J. Henley, *Chem. Soc. Rev.* (in press), and references therein.
- [25] D.P. Dowling, K. Donnelly, M. Monclus, M. McGuinness, *Diamond Relat. Mater.* 7 (1998) 432.
- [26] G.M. Fuge, C.J. Rennick, S.R.J. Pearce, P.W. May, M.N.R. Ashfold, *Diamond Relat. Mater.* 12 (2003) 1049.
- [27] Y.H. Cheng, X.L. Qiao, J.G. Chen, Y.P. Wu, C.S. Xie, Y.Q. Wang, et al., *Diamond Relat. Mater.* 11 (2002) 1511.
- [28] C.W. Ong, X.-A. Zhao, Y.C. Tsang, C.L. Choy, P.W. Chan, *Thin Solid Films* 280 (1996) 1.
- [29] X.-A. Zhao, C.W. Ong, Y.C. Tsang, K.F. Chan, C.L. Choy, P.W. Chan, et al., *Thin Solid Films* 322 (1998) 245.
- [30] M.E. Ramsey, E. Poindexter, J.S. Pelt, J. Marin, S.M. Durbin, *Thin Solid Films* 360 (2000) 82.
- [31] A.C. Ferrari, J. Robertson, *Phys. Rev. B* 61 (2000) 14 095.

- [32] H. Baranska, A. Labudzinska, J. Terpinski, in: R.A. Chalmers, M. Masson (Eds.), *Laser Raman Spectrometry*, John Wiley and Sons, New York, 1987, Chap. 4.
- [33] *Handbook of X-ray Photoelectron Spectroscopy*, Perkin–Elmer Corp, 1992.
- [34] R. Haerle, E. Riedo, A. Pasquarello, A. Baldereschi, *Phys. Rev. B.* 65 (2002) 045101.
- [35] P. Mérel, M. Tabbal, M. Chaker, S. Moisa, J. Margot, *Appl. Surf. Sci.* 136 (1998) 105.
- [36] F. Tuinstra, J.L. Koenig, *J. Chem. Phys.* 53 (1970) 1126.